

## Short Communication

# Single-Walled Carbon Nanotube Based Real-Time Organophosphate Detector

Ningyi Liu,<sup>b</sup> Xianpeng Cai,<sup>a</sup> Yu Lei,<sup>a,c\*</sup> Qing Zhang,<sup>b\*</sup> Mary B. Chan-Park,<sup>a</sup> Changming Li,<sup>a</sup> Wilfred Chen,<sup>d</sup> Ashok Mulchandani<sup>d</sup>

<sup>a</sup> School of Chemical and Biomedical Engineering, Nanyang Technological University, Nanyang Avenue, Singapore 639798  
\*e-mail: ylei@enr.uconn.edu

<sup>b</sup> School of Electrical and Electronic Engineering, Nanyang Technological University, Nanyang Avenue, Singapore 639798  
\*e-mail: eqzhang@ntu.edu.sg

<sup>c</sup> Department of Chemical, Materials and Biomolecular Engineering, University of Connecticut, 191 Auditorium Road, Unit 3222 Storrs, CT 06269-3222, USA

<sup>d</sup> Department of Chemical and Environmental Engineering, University of California, Riverside, CA 92521, USA

Received: September 28, 2006

Accepted: December 18, 2006

## Abstract

A novel single-walled carbon nanotube (SWNT) based biosensor for real-time detection of organophosphate has been developed. Horizontally aligned SWNTs are assembled to desirable electrodes using AC dielectrophoresis technique. Organophosphorus hydrolase (OPH) immobilized on the SWNTs by nonspecific binding triggers enzymatic hydrolysis of organophosphates (OPs), such as paraoxon, consequently causing a detectable change in the conductance of the SWNTs. The conductance change is found to be correlated to the concentration of organophosphate. Our results suggest the novel biosensor has great potential to serve as a simple and reusable platform of sensing organophosphate on a real-time basis.

**Keywords:** Carbon nanotubes, Organophosphorus hydrolase, Real-time, Biosensor, Bioelectronics

DOI: 10.1002/elan.200603761

Recently, one-dimensional nano-material carbon nanotubes (CNTs) have been explored intensively for various sensor applications. For example, taking advantage of its high surface/volume ratio, as well as its properties to enhance electrocatalytic activity and promote electron-transfer reactions, CNT has been used to modify electrochemical electrodes to detect various species, such as glucose [1, 2] and NADH [3]. On the other hand, because of efficient charge transfer between CNTs and surface-anchored molecules, CNTs, especially semiconducting single-walled carbon nanotubes (SWNTs), exhibit high sensitivity to variations of surrounding electrostatic environments. Therefore, except for those CNT-based electrochemical sensors, CNTs are also a promising material for electronic sensors, e.g., sensors based on the structure of CNT field effect transistor (CNTFET). These CNT based electronic sensors include gas sensors for nitrogen dioxide [4], ammonia [4, 5] and carbon dioxide [6], and biosensors for proteins [7–12], DNA hybridization [13], glucose [14] and etc. However, most of these biosensors developed are based on CNT conductance change induced by binding events, such as antigen-antibody binding and DNA hybridization.

Organophosphorous (OP) compounds are among the most toxic substances and they are thus commonly used as pesticides, insecticides and chemical warfare agents [15].

There has been growing demand of reliably on-site monitoring OP compounds. Common laboratory-based analytical techniques for detecting OP compounds primarily include either gas or liquid chromatography. Both processes are expensive and time-consuming [16]. In the past decade, biosensors based on inhibition of acetylcholine esterase (AChE) have been widely used for detecting OP compounds. Unfortunately, such inhibition biosensors typically have very poor selectivity and do not function on a real-time basis. They are only for single use due to the irreversible inhibition of enzyme activity. Recently, fast and direct detection of OPs is possible by applying the biocatalytic action of organophosphorous hydrolase (OPH), where OPs were used as the sensor substrates. As a result, OPH is extremely attractive for the potential application in detecting OP compounds [17]. The CNT-based OPH amperometric biosensors have been reported recently for organophosphates [18, 19], but they are still based on multi-walled carbon nanotubes (MWNTs) modified electrochemical detection.

In this paper we demonstrate the first OPH-functionalized SWNT based electronic biosensor for real-time OPs detection (Fig. 1). SWNTs are assembled to bridge electrode pairs using AC dielectrophoresis technique. Organophosphorous hydrolase (OPH) immobilized on the SWNTs by nonspecific binding triggers enzymatic hydrolysis of

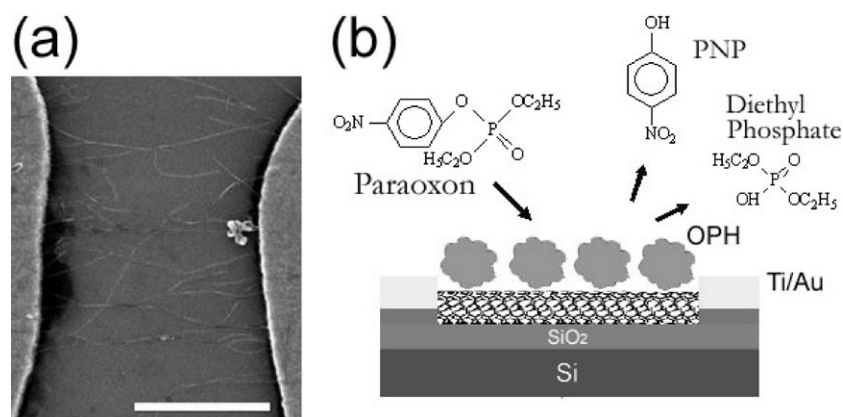


Fig. 1. a) SEM picture of a typical SWNT sensor. Well aligned SWNT networks connect the electrodes. The scale bar is 1  $\mu\text{m}$ . b) Schematic of paraoxon detection based on an OPH functionalized SWNT electronic sensor.

paraoxon, consequently causing a detectable real-time change in the conductance of the SWNTs. The fabrication, detection mechanisms, and advantages of the enzyme functionalized SWNT electronic sensor are discussed in detail in the following sections.

The nonspecific binding (NSB) of OPH on the SWNTs was confirmed by atomic force microscopy (AFM) images shown in Figure 2a. Before OPH immobilization, the height of the SWNTs was constant over its length. While, after OPH immobilization, the average height was found to increase from 3 to 5 nm. This increment in the height is in good agreement with OPH dimension of a few nanometers observed by Lei et al. [20]. The spontaneous adsorption of OPH is attributed to the strongly hydrophobic interaction between the SWNTs and enzyme [21–23].

OPH NSB can be further verified from the downward shift in the  $I-V_g$  curves of the SWNT sensors before and after OPH binding as shown in Figure 2b. The gate voltage  $V_g$  was applied to the silicon substrate. This phenomenon can be interpreted as follows. First of all, the adsorbed enzyme could induce a significant scattering potential and act as carrier scattering sites along the SWNTs [11], leading to a decrease in the conductance. Secondly, it has also been reported that protein adsorption can reduce the work function of gold electrodes [10]. As a result, the height of the Schottky barriers (SB) between the metallic electrode and SWNTs is increased and the resistance to hole transport in the SWNTs is also increased, thus a decrease in channel conductance. Electron donation of amine groups of OPH is the third possible mechanism [8]. The schematic of the SWNT sensors is shown in Figure 1b.

Preliminary result shown in Figure 3 suggests OPH-functionalized SWNT sensors are sensitive to paraoxon. In order to eliminate the influence of pH change on the conductance due to the enzymatic hydrolysis of paraoxon, all samples were prepared in 0.01 M pH 7.4 phosphate buffer solution and all measurements were conducted in the same buffer. The device was first wetted with 1  $\mu\text{L}$  buffer. The addition of 1  $\mu\text{L}$  buffer did not cause any significant conductance change of the wetted SWNT sensors. However,

when 1  $\mu\text{L}$  of 50  $\mu\text{M}$ , 200  $\mu\text{M}$  and 1 mM paraoxon in phosphate buffer was injected using a pipette, the conductance of the sensors showed a rapid decay to a new saturated conductance. Figure 3 inset showed the relative conductance change of the device as a function of calculated final concentration of paraoxon. The nonlinear response to

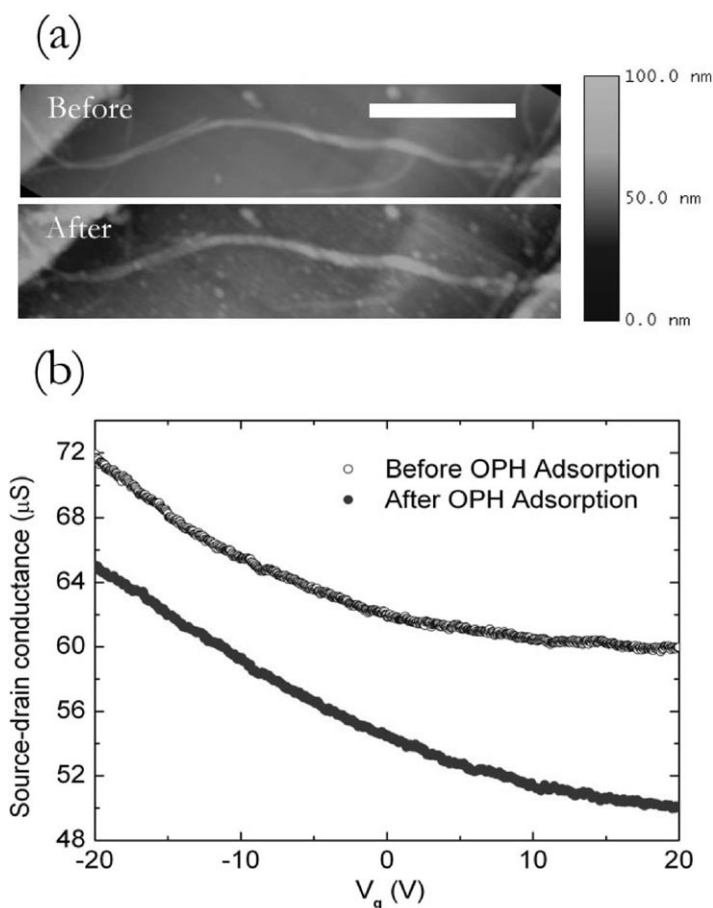


Fig. 2. a) AFM images of a typical SWNT sensor before and after OPH immobilization. The scale bar is 1  $\mu\text{m}$ . b)  $I-V_g$  curves of the SWNT sensor before and after OPH immobilization.

paraoxon concentration might be attributed to saturation kinetics of enzymatic reaction. After the device was heated at 80°C for 1 h to inactivate the enzyme, it showed an insignificant response to 1 mM paraoxon (Figure 3 inset b). Additionally, the as-prepared CNTFET without immobilized OPH showed an insignificant response to 1 mM paraoxon as well (Figure 3 inset c). Both of control experiments suggest that OPH does play a key role in the detection of paraoxon. We also test the re-usability of the devices. The responses of another OPH functionalized SWNT sensor to the buffer and paraoxon buffer solution, respectively, were examined and they showed similar characteristics as the previous device (Figure 4). After the device was rinsed and blown dry with N<sub>2</sub>, the second round of measurement was conducted. One can see that before paraoxon addition, the baselines of the two round experiments were nearly overlapped. Interestingly, the device was still active to respond to paraoxon in the second round test. In comparison with the first round, the relatively small and slow response could be caused by the fact that some noncovalently immobilized OPH molecules were washed away during rinsing process before the second round detection.

The mechanism of the conductance decreasing with paraoxon addition is still under investigation. We suppose that the sensing signal may come from the hydrolyzed products, or OPH molecules themselves. OPH hydrolyzes paraoxon to generate *p*-nitrophenol (PNP) and diethyl phosphate. According to our experimental results elsewhere [24], PNP increases the conductance while diethyl phosphate decreases the conductance. Interestingly, the mixture of same concentration of PNP and diethyl phosphate only cause a decrease in the conductance. From these observations, we hypothesize that hydrolyzed products could

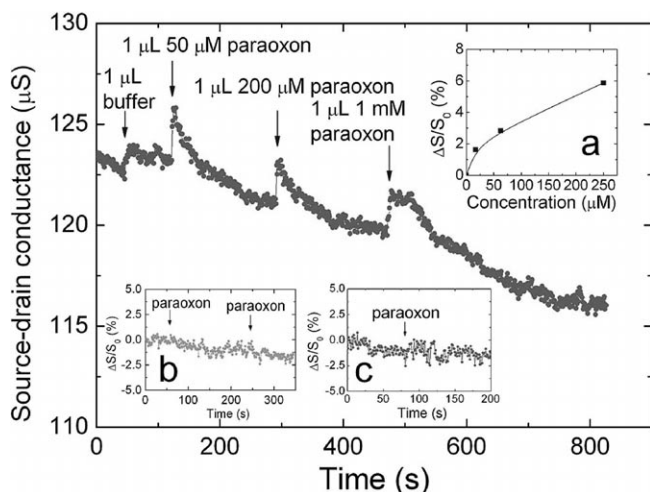


Fig. 3. Real-time response of an OPH functionalized SWNT sensor to phosphate buffer and different concentrations of paraoxon. The SWNT channel of the sensor was immersed in 1  $\mu\text{L}$  buffer initially. The p-type silicon was connected to ground. Inset (a) shows relative conductance change of the device as a function of OP concentration. Inset (b) shows the response of a device with inactive OPH. Inset (c) shows the response of as-prepared CNTFET without OPH to paraoxon.

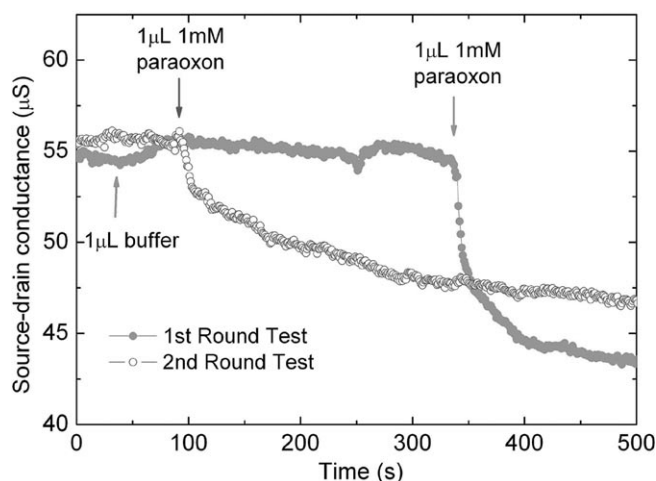


Fig. 4. The response of another OPH functionalized SWNT sensor to phosphate buffer and paraoxon. After the first round test, the device was rinsed and blown dry with nitrogen. Before the second round real-time measurement, 1  $\mu\text{L}$  phosphate buffer was used to wet the SWNT channel. The p-type silicon was connected to ground.

contribute to the conductance change. Furthermore, it has been suggested that in the catalytic reaction OPH undergoes deformation [14], resulting the change of charge status on the surface of enzyme. This deformation could not only affect charge transfer of enzyme molecules to the bulk part of SWNTs, but also further change the height of SB at the contact region between SWNTs and metallic electrodes, since CNTFET is basically a SB-FET [25] and the adsorbates on the contact region may affect the conductance of CNTFET through SB height modulation. Since the exact mechanisms of OPs detection by OPH functionalized CNTFET are not clear yet, more experiments with optimized device structure are needed, for example, control experiments on devices with only contact region or channel region exposed so that the effects of contact part and bulk part of SWNTs during the OPs sensing could be distinguished.

In conclusion, we have demonstrated a novel biosensor for real-time organophosphate detection using enzyme as the molecular recognition elements and SWNT bundles as the transducer. The real-time electrical conductance response of the sensors to the addition of paraoxon is attributed to the enzymatic hydrolysis. Changes of charge status of enzyme and the “electron” or “hole” doping effect of enzymatically hydrolyzed products are likely to be the dominant factors for the conductance response. Compared to the electrochemical detection method, the novel biosensors could serve as a simple and low-cost platform with real-time and re-usability biosensing capability.

### Experimental

1 mg commercial SWNTs with 95% purification (MER Inc.) were firstly suspended in 100 mL deionized water with 1 wt% sodium dodecyl sulfate (SDS). The suspension was

ultra-sonicated for 2 h, followed by centrifuged at 10000 rpm for 1 h. The upper 80% of the suspension was decanted for the second round of centrifugation. After that, the well-dispersed suspension was ready for connecting the SWNTs to the electrodes. The SWNT sensors were fabricated on p-type silicon wafers with a 500 nm thick SiO<sub>2</sub> layer. A pair of 20-nm Ti/40-nm Au electrodes was patterned on the SiO<sub>2</sub> layer using conventional e-beam deposition and photo-lithography processes. AC dielectrophoresis method was used to assemble SWNTs to the electrode pairs [26, 27]. After a 2  $\mu$ L droplet of the SWNT suspension was introduced to the device area, an AC bias with 10 V peak-to-peak voltage at a frequency of 6 MHz was applied for 1 min. In order that the biomaterials can well adsorb on the surface of the SWNTs, the devices were rinsed with deionized water and soaked in it for overnight to completely remove SDS residuals [28, 29]. Selective electrical burnout [30] process was applied to remove metallic SWNTs and ensure a better electric contact between the semiconducting SWNTs and electrodes. From Figure 1a, one can see well aligned SWNT bundles bridging the electrode pairs. Organophosphorous hydrolase was used to functionalize the SWNT bundles through nonspecific binding. A trace volume of OPH solution (in 0.01 M pH 7.4 phosphate buffer) was introduced onto the SWNTs by a pipette. After one hour the samples were rinsed with deionized water to remove unbound enzyme and buffer residuals and dried with nitrogen. The electrical properties of the SWNT sensors were characterized using a precise semiconductor parameter analyzer (HP 4156B) at room temperature. During the measurements, the voltage difference between the electrodes was kept at 200 mV.

#### Acknowledgements

We greatly appreciate NTU/NanoCluster and BPE Cluster for supporting studies on this project. The authors also thank Hong Li and Ning Peng for helpful discussion.

#### References

- [1] S. B. Hocevar, J. Wang, R. P. Deo, M. Musameh, B. Ogorevc, *Electroanalysis* **2005**, *17*, 417.
- [2] S. G. Wang, Q. Zhang, R. Wang, S. F. Yoon, J. Ahn, D. J. Yang, J. Z. Tian, J. Q. Li, Q. Zhou, *Electrochem. Commun.* **2003**, *5*, 800.
- [3] M. Musameh, J. Wang, A. Merkoci, Y. Lin, *Electrochem. Commun.* **2002**, *4*, 743.
- [4] P. Qi, O. Vermesh, M. Grecu, A. Javey, Q. Wang, H. Dai, S. Peng, K. J. Cho, *Nano Lett.* **2003**, *3*, 347.
- [5] K. Bradley, J.-C. P. Gabriel, M. Briman, A. Star, G. Gruner, *Phys. Rev. Lett.* **2003**, *91*, 218301.
- [6] A. Star, T.-R. Han, V. Joshi, J.-C. P. Gabriel, G. Gruner, *Adv. Mater.* **2004**, *16*, 2049.
- [7] A. Kojima, C. K. Hyon, T. Kamimura, M. Maeda, K. Matsumoto, *Jpn. J. Appl. Phys.* **2005**, *44*, 1596.
- [8] K. Bradley, M. Briman, A. Star, G. Gruner, *Nano Lett.* **2004**, *4*, 253.
- [9] R. J. Chen, S. Bangsaruntip, K. A. Drouvalakis, N. W. S. Kam, M. Shim, Y. Li, W. Kim, P. J. Utz, H. Dai, *Proc. Natl. Acad. Sci. U.S.A.* **2003**, *100*, 4984.
- [10] R. J. Chen, H. C. Choi, S. Bangsaruntip, E. Yenilmez, X. Tang, Q. Wang, Y. Chang, H. Dai, *J. Am. Chem. Soc.* **2004**, *126*, 1563.
- [11] A. Star, J.-C. P. Gabriel, K. Bradley, G. Gruner, *Nano Lett.* **2003**, *3*, 459.
- [12] H.-M. So, K. Won, Y. H. Kim, B.-K. Kim, B. H. Ryu, P. S. Na, H. Kim, J.-O. Lee, *J. Am. Chem. Soc.* **2005**, *127*, 11906.
- [13] A. Star, E. Tu, J. Niemann, J.-C. P. Gabriel, C. S. Joiner, C. Valcke, *Proc. Natl. Acad. Sci. U.S.A.* **2006**, *103*, 921.
- [14] K. Besteman, J.-O. Lee, F. G. M. Wiertz, H. A. Heering, C. Dekker, *Nano Lett.* **2003**, *3*, 727.
- [15] S. Chapalamadugu, G. S. Chaudry, *Crit. Rev. Biotechnol.* **1992**, *12*, 357.
- [16] J. Sherma, *Anal. Chem.* **1993**, *65*, 40.
- [17] A. Mulchandani, W. Chen, P. Mulchandani, J. Wang, K. R. Rogers, *Biosens. Bioelectron.* **2001**, *16*, 225.
- [18] R. P. Deo, J. Wang, I. Block, A. Mulchandani, K. A. Joshi, M. Trojanowicz, F. Scholz, W. Chen, Y. Lin, *Anal. Chim. Acta* **2005**, *530*, 185.
- [19] K. A. Joshi, M. Prouza, M. Kum, J. Wang, J. Tang, R. Haddon, W. Chen, A. Mulchandani, *Anal. Chem.* **2006**, *78*, 331.
- [20] C. Lei, Y. Shin, J. Liu, E. J. Ackerman, *J. Am. Chem. Soc.* **2002**, *124*, 11242.
- [21] R. J. Chen, Y. Zhang, D. Wang, H. Dai, *J. Am. Chem. Soc.* **2001**, *123*, 3838.
- [22] Y. Lin, L. F. Allard, Y.-P. Sun, *J. Phys. Chem. B* **2004**, *108*, 3760.
- [23] M. Shim, N. W. S. Kam, R. J. Chen, Y. Li, H. Dai, *Nano Lett.* **2002**, *2*, 285.
- [24] X. Cai, N. Liu, Y. Lei, Q. Zhang, unpublished results.
- [25] P. Avouris, J. Appenzeller, R. Martel, S. J. Wind, *Proc. IEEE* **2003**, *91*, 1772.
- [26] J. Li, Q. Zhang, N. Peng, Q. Zhu, *Appl. Phys. Lett.* **2005**, *86*, 153116.
- [27] N. Peng, Q. Zhang, J. Li, N. Liu, *J. Appl. Phys.* **2006**, *100*, 024309.
- [28] Z. Zhang, J. Cardenas, E. E. B. Campbell, S. Zhang, *Appl. Phys. Lett.* **2005**, *84*, 043110.
- [29] L. Dong, V. Chirayos, J. Bush, J. Jiao, V. M. Dubin, R. V. Chebrian, Y. Ono, J. John F. Conley, B. D. Ulrich, *J. Phys. Chem. B* **2005**, *109*, 13148.
- [30] J. Li, Q. Zhang, D. Yang, J. Tian, *Carbon* **2004**, *42*, 2263.